REPORT DOCUMENTATION PAGE

Form Approved
OMB No. 0704-0188

1. AGENCY USE ONLY (Leave blank)	2. REPORT DATE	3. REPORT TYPE AND DATES COVERED
	May 31, 1988	March 15, 86 - June 13, 86

4. TITLE AND SUBTITLE

Semiconductor Engineering for High-Speed Devices.

5. FUNDING NUMBERS

F49620-85-C-0103

6. AUTHOR(S)

A. Sher, S. Krishnamurthy and A.-B. Chen

7. PERFORMING ORGANIZATION NAME(S) AND ADDRESS(ES)

Advanced Research Projects Agency
1400 Wilson Boulevard
Arlington, VA 22209

8. PERFORMING ORGANIZATION REPORT NUMBER

9. SPONSORING / MONITORING AGENCY NAME(S) AND ADDRESS(ES)

US Air FOrce.

10. SPONSORING / MONITORING AGENCY REPORT NUMBER

11. SUPPLEMENTARY NOTES

12a. DISTRIBUTION / AVAILABILITY STATEMENT

Approved for public release;
distribution unlimited.

12b. DISTRIBUTION CODE

13. ABSTRACT (Maximum 200 words)

14. SUBJECT TERMS

15. NUMBER OF PAGES

16. PRICE CODE

17. SECURITY CLASSIFICATION OF REPORT	18. SECURITY CLASSIFICATION OF THIS PAGE	19. SECURITY CLASSIFICATION OF ABSTRACT	20. LIMITATION OF ABSTRACT
Unclassified	Unclassified	Unclassified	Unclassified

NSN 7540-01-280-5500

Standard Form 298 (890104 Draft)
Prescribed by ANSI Std. Z39-18
298-01

SRI International

SEMICONDUCTOR ENGINEERING FOR HIGH-SPEED DEVICES

Quarterly R&D Status Report No. 4

Covering the Period 15 March 1986 to 13 June 1986

13 June 1986

By:

A. Sher Principal Investigator, (415) 859-4466
S. Krishnamurthy and A.-B. Chen
Physical Electronics Laboratory

Prepared for:

Air Force Office of Scientific Research
Bolling Air Force Base, D.C. 20332-6448

Advanced Research Projects Agency (DOD)
1400 Wilson Boulevard
Arlington, Virginia 22209

Attn: Captain Kevin Malloy, Program Manager
(202-767-4984)

SRI Project 8725
ARPA Order 5396, Program Code 5D10
Contract F49620-85-C-0103
Effective Date: 1 June 1985
Contract Expiration Date: 31 May 1988
Contract Dollars: $611,296

SRI International
333 Ravenswood Ave • Menlo Park, CA 94025
415 326-6200 • TWX 910-373-2046 • Telex 334-486

I DESCRIPTION OF PROGRESS

This report summarizes major accomplishments covering the period 15 March to 13 June. A paper entitled "Velocity Field Characteristics of III-V Semiconductor Alloys" which was submitted to the Journal of Applied Physics is attached as Appendix A.

Our aim in this period has been to expand the work reported in Appendix A to study the effect of ionized impurity scattering and strain scattering on the electron mobility. The modified electron mobility will, in turn, affect velocity-field (v-E) characteristics in semiconductors and their alloys.

Ionized impurity scattering is treated in a second order perturbation theory. Our improvement over previous theories is to convert the usual integration over a parabolic energy band to a general Brillioun Zone (BZ) integration. This conversion allows us to incorporate the effect of realistic band structures into this transport calculation.

We modeled the strain scattering so the scattering parameters are calculated from the empirical pseudopotential form factors used in the band structure calculation. The improvement over previous models stems from the universal nature of the scattering parameters.

The VCA band structures have been used to obtain group velocity as a function of momentum and crystal orientation in various alloys. The group velocity curve can be used to judge the optimum electron energy and momentum to inject into ballistic devices. Moreover, the net scattering time due to all mechanisms can be calculated as a function of electron energy. The energy dependent mean-free path is the product of the group velocity and these scattering times. These mean-free paths set an upper limit on the length of the active region in a ballistic transport device for a given orientation.

Results:

(1) The effect of band structure and the more accurate BZ integration are found to be substantial electron densities, n, in excess of 10^{17} cm^{-3}. At $n = 10^{18}$ cm^{-3}, band structure effects alone reduce the electron mobility by about 25% relative to those calculated in the constant effective mass approximation for an electron temperature of 1000 K. This effect needs to be included in any accurate calculation of v-E behavior.

(2) Calculations of group velocity from VCA band structure suggest InAs or InSb compounds will be better suited to ballistic electron devices than GaAs. As seen from the enclosed curves, the maximum group velocity always occurs in the (100) directions, and InAs is about 70% larger than that in GaAs. Recent experiments [Levi, et al., Appl.

Phys. Lett., (1986) to be published] also find that InAs-based devices are about 7 times more efficient than those based on GaAs. We still must calculate these effects including the full CPA band structures. Our calculations further show that v_g in (100) is larger than that in either (110) or (111).

Because CRAY time is now available, we are now engaged in calculation of CPA band structures of various alloys. The effect of real part of self energy will change the density of states and group velocities at higher energies. These changes will be included in the calculation of alloy, impurity, strain and phonon scattering. Also these calculations will include anisotropic scattering. Then, the peak velocity and the saturation velocity will be obtained for various alloys.

II EQUIPMENT PURCHASED OR CONSTRUCTED

None

III TRIPS, MEETINGS, PAPERS, AND VISITS

Dr. Arden Sher and Srinivasan Krishnamurthy attended an American Physics Society Conference in Las Vegas, Nevada, March 31 to April 4, 1986. The following paper has been submitted to Journal of Applied Physics: "Velocity-Field Characteristics of III-V Semiconductor Alloys," by S. Krishnamurthy, A. Sher, and A.-B. Chen.

IV PROBLEMS OR AREAS OF CONCERN

None

V DEVIATION FROM PLANNED EFFORT

None

VI FISCAL STATUS

The total contract funding for the three-year period is $611,296. Of this, $195,287 was allocated to the first year. Including the burden, approximately $22,000 was intended to pay the consulting fee of An-Ban Chen leaving approximately $173,000. In the first year ending 31 May 1986, we spent approximately $192,000. Year two has been allocated $203,655, with $20,284 intended to pay the consulting fee of An-Ban Chen.

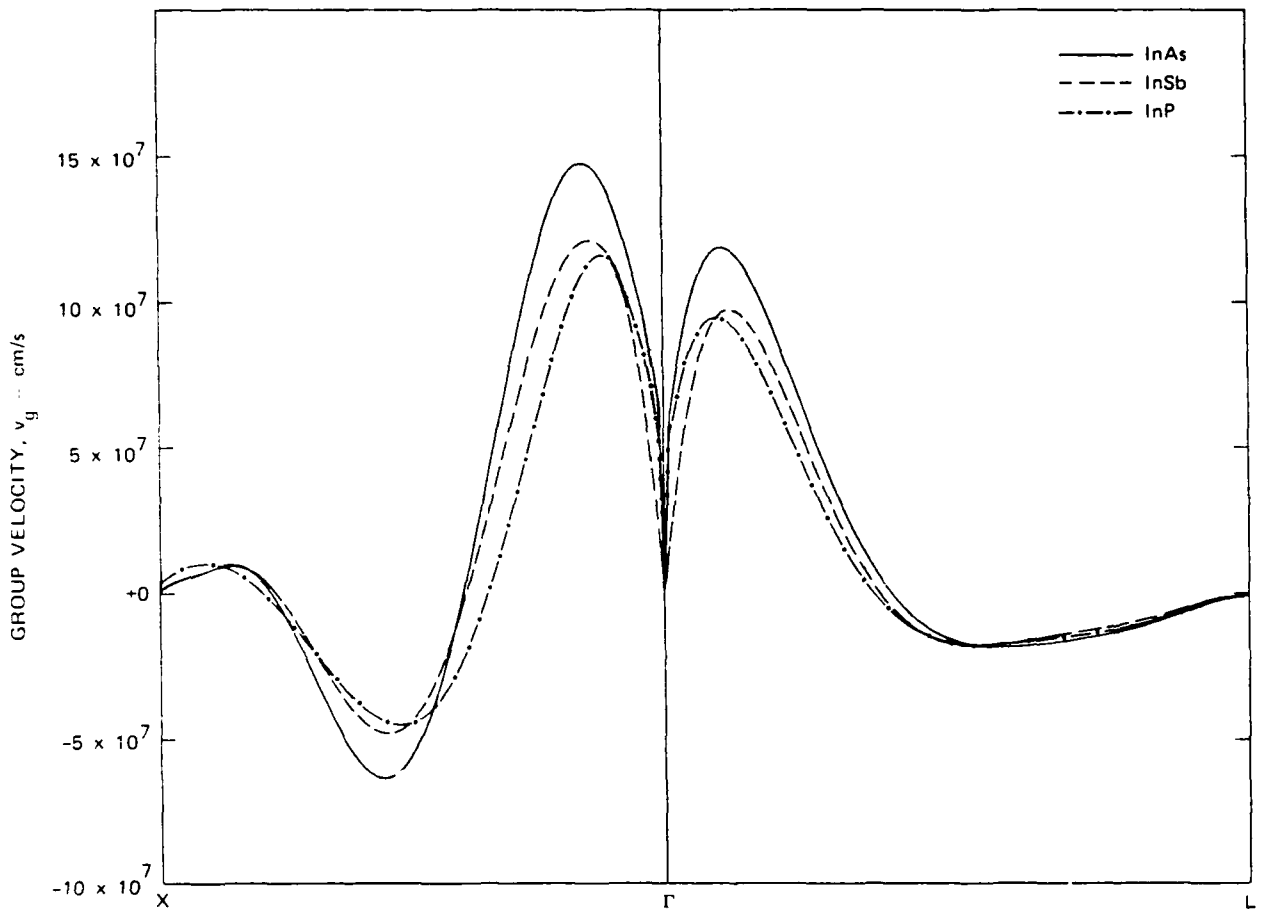
InAs
InSb
InP
15 x 10^7
10 x 10^7
5 x 10^7
+0
-5 x 10^7
-10 x 10^7
GROUP VELOCITY, v_g — cm/s
X
Γ
L

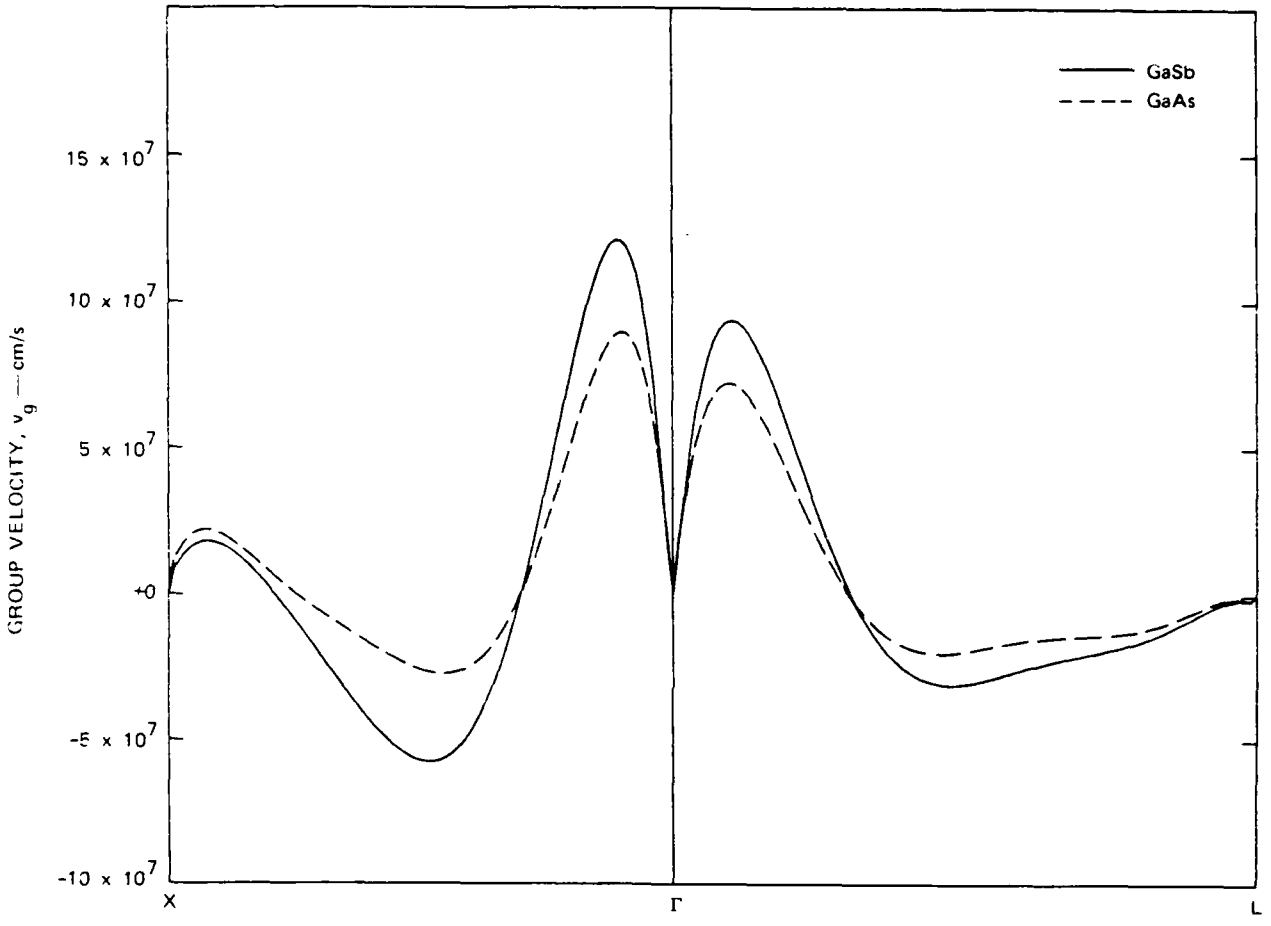
GaSb
GaAs
15 x 10^7
10 x 10^7
5 x 10^7
+0
-5 x 10^7
-10 x 10^7
GROUP VELOCITY, v_g — cm/s
X
Γ
L

APPENDIX A

VELOCITY-FIELD CHARACTERISTICS OF III-V SEMICONDUCTOR ALLOYS

May 1986

By: Srinivasan Krishnamurthy and A. Sher
Physical Electronics Laboratory

A.-B. Chen
Department of Physics
Auburn University

Submitted to *Journal of Applied Physics*

Velocity-field characteristics of III-V semiconductor alloys

Srinivasan Krishnamurthy and A. Sher

Physical Electronics Laboratory

SRI International, Menlo Park, California 94025

A.-B. Chen

Department of Physics

Auburn University, Auburn, Alabama 36801

(Received:

ABSTRACT

We have calculated the velocity-field characteristics of semiconductor alloys based on realistic band structures; we obtained the band structures and alloy-scattering rates from a generalization of the coherent potential approximation method. Although we use proper band structures, we still consider a single electron-temperature model. The results agree surprisingly well with experiments, and suggest that InP-based alloys are good candidates for high-speed devices.

I. INTRODUCTION

In many semiconductors, the electron drift velocity, v, increases nonlinearly under the influence of high fields to reach a peak value, v_p, at a threshold field, E_T, and then decreases with applied E, giving rise to a negative differential resistance. For device applications, one must know the effect of material (band-structure) parameters on hot electron transport. In this paper, we examine the influence of the band-structure effects on velocity-field characteristics of III-V ternary alloys. Such information, calculated differently, is already available for several III-V and II-VI compounds and some alloys.[1,2,3] Our improvement over previous efforts is to use accurate band structures and alloy scattering rates for many systems. Our aim is to examine systematically the factors which limit the values of E_T and v_p and to suggest likely materials for high-speed device applications.

II. MODEL FOR v-E CHARACTERISTICS

For this comparative study, we have adopted a simple hot electron theory[2] that assumes a "drifted Maxwellian" electron distribution with a single electron temperature, T_e. This distribution would be established only if there were an interaction, like electron-electron scattering, that drove the electron system into internal equilibrium at a rate fast compared to the rate of energy exchange with the heat bath.[4] No such interaction has ever been identified because it requires very high electron density. Nevertheless, the predictions of the drifted Maxwellian distribution are surprisingly accurate, and it serves as a good vehicle for this systematic study, so we are adopting it in this paper.

Under high field, the electrons gain energy when they are accelerated from the conduction band minimum to higher energy levels. The average electronic energy in a steady state is often considerably higher than that of the lattice excitation energy per particle. The electron temperature, T_e, which represents the average electron energy, is therefore much higher than the lattice temperature, T. For a direct-gap semiconductor,

the mobility in the lower valley, μ_1, is much larger than that in the higher valleys, μ_2, so the drift velocity can be approximated by[2]

$$v = \mu_1 E/(1+Re^{-\Delta E/kT_e}) \quad , \tag{1}$$

where R is the ratio between the densities of states in the upper and lower valleys, respectively, and ΔE is the energy difference between the minima of these two valleys. In steady state, the energy gained by an electron from the field must be balanced by the energy lost to the lattice

$$evE = (3/2)\ k(T_e - T)/\tau_E \quad , \tag{2}$$

where τ_E is the electron-lattice energy relaxation time. Equations (1) and (2) combine to yield T_e, which in turn yields the v-E characteristic curve and hence the threshold values E_T and v_p. These values have the following approximate forms: $v_p \propto \sqrt{\mu_1 \Delta E/\tau_E}$ and $E_T \propto \sqrt{R\Delta E/\mu_1 \tau_E}$.

Alloy effects come not only from the concentration dependence of the band parameters R and ΔE, but also from the effect of alloy scattering on the mobility. We take μ_1 to be

$$\mu_1^{-1} = \mu_0^{-1}\ (T) + \mu_A^{-1}\ (T_e) \quad ,$$

where μ_0 is the mobility limited by all scattering mechanisms except alloy scattering and is taken as the concentration-weighted average of the experimental values of the two constituent compounds. μ_A is the alloy-scattering-limited mobility and is calculated using a generalized Brooks' formula.[5]

Finally, we assume that electrons lose energy to the lattice mainly through polar optical phonon scattering and calculate τ_E from Eq. (3.6.26) of Ref. 1. The electronic and lattice parameters needed for this estimate are all taken to be the concentration-weighted averages of the pure crystal constituents.

III. BAND STRUCTURES

To calculate the alloys' band structures, we must begin with those of the pure compounds. We have demonstrated[6] that high-quality band structures for II-VI and III-V compounds can be obtained using a minimum set of four sp^3 Slater orbitals per atom in a semi-empirical calculation. First, the empirical pseudo-potential form factors are used to construct a tight-binding (TB) Hamiltonian H in this minimum set. H is then transformed into a zeroth order H_0 in an orthonormal basis. Then a perturbative Hamiltonian having a first-neighbor TB form and a site-diagonal spin-orbit Hamiltonian are added to obtain a fine-tuned band structure. This band structure accurately reproduces the energy separation between the lowest and the next lowest minima in the conduction bands, the band gap E_g, and the conduction band effective mass m^*.

Figure 1 shows an example of a band structure for InAs. The quality of the band structure can be seen to be comparable to the best ones available.[7] The band structure obtained in this way is superior to the results of the usual first- or second-neighbor TB approach because our method includes all the long-range interactions. Figures 2(a) and 2(b) show the lowest conduction band in ΓX and ΓL directions for InAs, InSb, InP and GaAs, GaSb compounds, respectively. The phenomena we are examining are only sensitive to energy variation of states relative to the conduction minima, so all the curves are drawn with their conduction band edges aligned. Because the InP, InSb conduction bands cross in Figure 2(a), their alloys will have larger μ_1 but smaller ΔE than does InP. The peak velocity in these alloys can be larger than that of InP. However, both μ_1 and ΔE will be larger in InPAs alloys than that in InP. One can expect a moderate increase

in v_p and E_T^{-1}. Because μ_1 and ΔE are almost the same in GaAs and GaSb, electron-phonon interactions then determine the change in v-E characteristics.

Table I lists the important band parameters of the six pure III-V compounds included in this study. Also included is the minimum energy a hot electron needs to create an electron-hole pair,[8] $E_g(1+2\alpha)/(1+\alpha)$, where α is the ratio of the electron mass to the heavy-hole mass.

These pure-crystal band structures are the input to the alloy electronic structure calculation using the coherent potential approximation (CPA).[9] Both diagonal disorder due to atomic term value differences and off-diagonal disorder due to bond-length fluctuations are treated. The method is a generalization of the tight-binding "molecular CPA" of Hass et al.[9] to our better band structures. From the CPA self-energy, one can obtain the alloy band gap, m^*, ΔE, R, and μ_1 as a function of the alloy concentration x. These quantities are then used to calculate the v-E characteristics as we described in Section II.

IV. EXAMPLE: $Ga_xIn_{1-x}As$

As an example, we present the results of our calculations for $Ga_xIn_{1-x}As$ in some detail in this section. Figure 3 plots ΔE, E_p, and v_p at two temperatures as a function of x. If ΔE is larger than E_p, avalanche breakdown is expected to occur before v_p is reached. Thus, the velocity-field plot near v_p is only meaningful for the range of x where $\Delta E < E_p$. The maximum value of v_p that can be obtained for this alloy is at $x \simeq 0.47$. The peak velocity, v_p, is seen to be a nonlinear function of x. Experimental[11] values of v_p (open circle) are also plotted.

Because we set the mobility of the satellite valley equal to zero in Eq. (1), we should not expect the model to be accurate for electric fields much higher than E_T. Nevertheless, it is interesting to examine the v-E curves produced by the model for different x values shown in Fig. 4. Because the mobility of InAs is larger than that of

GaAs, the slope in the low field region decreases with x. For the same reason, E_T increases with x. This prediction of a larger v_p value and a smaller E_T at lower GaAs content has been observed experimentally.[11] At x = 0.47, the v_p value is about 50% larger than that of GaAs, once again in agreement with experiments.[10,11]

The effect of the lattice temperature on the v-E characteristics is illustrated in Fig. 5. The curve sharpens at low T and the v_p value increases, because both μ_0 and μ_A are larger at lower T.

Figure 6 depicts two effects: the influence of alloy scattering on the v-E characteristics and the errors caused by the effective mass approximation (EMA). All three curves are for x = 0.5 and at T = 300 K. Curve (a) does not include alloy scattering and curve (c) does, but both are based on EMA. The presence of alloy scattering reduces the effective mobility, so curve (c) starts with a smaller slope and has a smaller v_p and a long tail as it approaches v_p, causing its E_T to be larger than curve (a). The reduction of v_p by alloy scattering in this case is about 30%. Curve (b) represents the results of a more detailed calculation using the actual density of states (DOS). Instead of Eq. (1), the drift velocity in this calculation is obtained from $v = \sigma E/(ne)$, where n is the electron density and σ is given by

$$\sigma = (2/3)e^2 \int \nu^2(\epsilon)\tau(\epsilon)\,(-\partial f/\partial\epsilon)d\epsilon \quad , \tag{3}$$

with $\tau(\epsilon)$ being the average momentum collision time, f the electron distribution, and ν^2 the energy-shell average of the square of the group velocity

$$\nu^2(\epsilon) = \sum_{nk} |\vec{v}_n(k)|^2\, \delta[\epsilon - \epsilon_n(k)] \quad . \tag{4}$$

Thus curve (b) does not assume a zero mobility for the higher valleys as was assumed in curves (a) and (c). We therefore infer that the effective mobility in curve (b) lies between those of curves (a) and (c). Comparison between curves (b) and (c) shows that the more elaborate calculation tends to have a moderate increase in v_p and a small reduction in E_T, largely because the bands increase with k more rapidly than quadratically before they bend over toward the satellite valley. Thus as a function of k, the effective mass actually first becomes smaller, then larger until the inflection point is reached, where the curvature changes sign and the effective mass becomes negative. The alloy mobility varies roughly as $(m^*)^{-5/2}$, so the net effect of the smaller m^* in the critical region is to produce curve (b). Moreover, the real part of the alloy scattering self-energy must also play a role, because it too modifies the energy bands. Thus, Monte Carlo calculations, which treat scattering on fixed energy band structures, cannot be expected to reproduce the same numerical result.

V. OTHER TERNARY ALLOYS

We have carried out the above calculations for the direct-gap ternary alloys GaInSb, InAsP, InAsSb, GaAsSb, and InPSb. The results are summarized in Fig. 7, the quantities plotted are the values of $\tilde{v}_p$ and $\tilde{E}_T^{-1}$, which are respectively the v_p and E_T^{-1} normalized to GaAs values. Also plotted are the values of ΔE and E_p. Because only a few alloys satisfy the condition $E_p > \Delta E$, the peak values, v_p, shown can actually be reached before avalanche breakdown takes place. The circles are the available experimental values[2,10,11] for v_p. Considering the simplifications involved in the model, the agreement with experiment is remarkable.

It is interesting to note that v_P is greater in InPSb than in pure InP and InSb, although alloy scattering tends to reduce v_p. Similar results are also seen in InPAs alloy. These results can be explained as follows: the phonon scattering rate in InP is larger than that in either InSb or InAs However, because of its larger effective mass, the mobility in InP is much smaller than those in InSb or InAs. The combined effect gives

rise to a larger v_p for the alloys. The ratio of the peak velocity to the energy dissipated by an electron traveling at this velocity is E_T^{-1}, and so $\tilde{E}_T^{-1}$ measures the efficiency of an alloy relative to GaAs in high-speed device applications. Our calculation of $\tilde{E}_T^{-1}$ also agrees very well with the available experimental data.

VI. SUMMARY

We have carried out a comparative evaluation of the influence of band structure features of several III-V compound alloys on velocity-field characteristics using detailed band structures and alloy scattering rates. Our results suggest that InP-based alloys are even more promising candidates for high-speed devices than GaAs. A more rigorous study is in progress to improve the accuracy of our calculations and further check this prediction.

ACKNOWLEDGMENT

This work was supported by DARPA contract F49620-85-C-0103.

FIGURE CAPTIONS

1. Band structure of InAs. Energy in eV.

2. Lowest conduction band of (a) InP, InAs, InSb and (b) GaAs, GaSb compounds. All energies measured in eV with respect to their respective conduction band minima.

3. Variation of ΔE, E_p, v_p as a function of GaAs concentration, x in $Ga_xIn_{1-x}As$ alloys. Experimental values (open circle) of v_p are from Ref. 11.

4. Velocity-field characteristics of $Ga_xIn_{1-x}As$ alloys.

5. Temperature dependence of v-E characteristics of $Ga_{0.5}In_{0.5}As$ alloy

6. Effect of band structure and alloy scattering on v-E characteristics. Results of the calculations (a) in EMA without alloy scattering, (b) in EMA with alloy scattering, and (c) with exact DOS and alloy scattering.

7. Variations of ΔE (solid line—in lower half), E_p (dotted line—in lower half), $\tilde{v}_p$ (solid line—in upper half), and $\tilde{E}_T^{-1}$ (dotted line—in upper half) are shown. $\tilde{v}_p$, $\tilde{E}_T^{-1}$ are peak velocity and threshold field in the unit of respective GaAs values. The experimental values of peak velocity (open circle) and threshold fields (filled circle) are also shown.

REFERENCES

[1]E.M. Conwell, *Solid State Physics*, Vol. 9 (Academic Press) (1967) and references cited therein.

[2]S.M. Sze, *Physics of Semiconductor Devices*, p. 645 (John Wiley & Sons, New York) (1978) and references cited therein.

[3]J.R. Hauser, M.A. Littlejohn, and T.H. Glisson, Appl. Phys. Lett., **28**, 458 (1976).

[4]A. Sher and H. Primakoff, Phys. Rev., **130**, 1267 (1963).

[5]S. Krishnamurthy, A. Sher, and A.-B. Chen, Appl. Phys. Lett., **47**, 160 (1985).

[6]A.-B. Chen and A. Sher, Phys. Rev., **B16**, 3572 (1977).

[7]J.R. Cheliskowsky and M.L. Cohen, Phys. Rev., **B14**, 556 (1976) and references cited therein.

[8]*Handbook of Physics*, 2nd edition (1972) (AIP).

[9]K.C. Hass, R.J. Lampart, and H. Ehrenreich, Phys. Rev. Lett., **52**, 77 (1984).

[10]T.H. Windhorn, L.W. Cook, and G.E. Stillman, J. Elec. Mater., **11**, 1065 (1982); IEEE Elec. Dev. Lett., EDL-3, 18 (1982).

[11]W. Kowalsky and A. Schlachetzki, Solid-State Electron., **28**, 299 (1985).

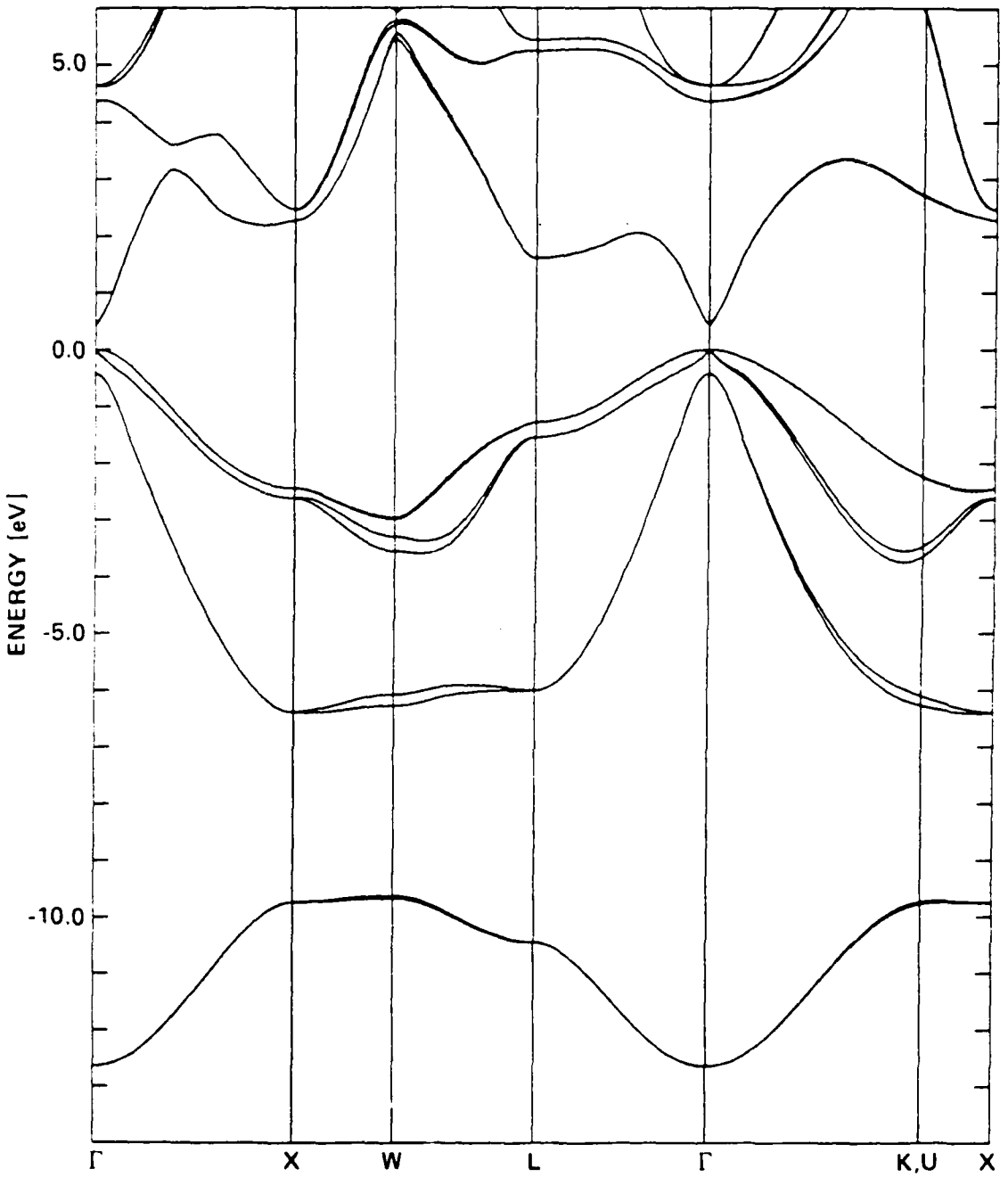

FIGURE 1

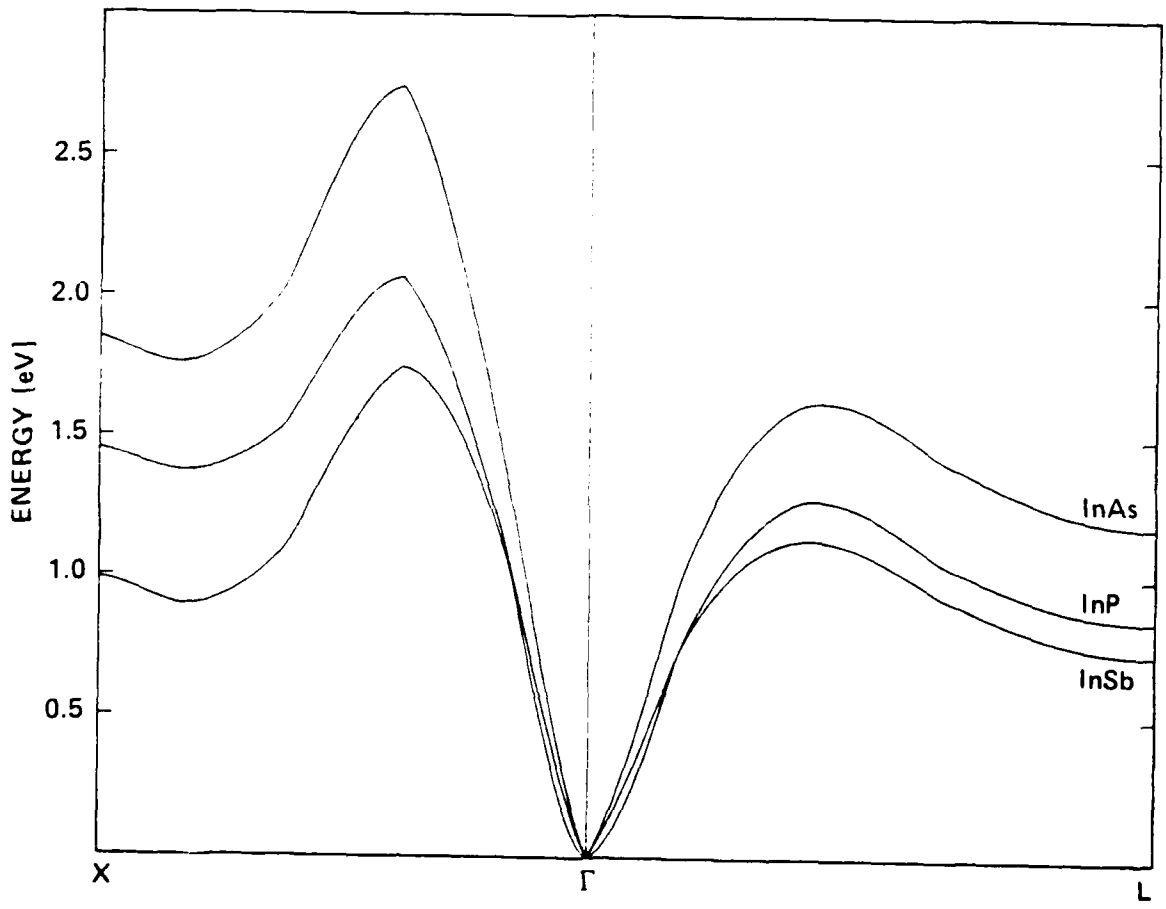

FIGURE 2a

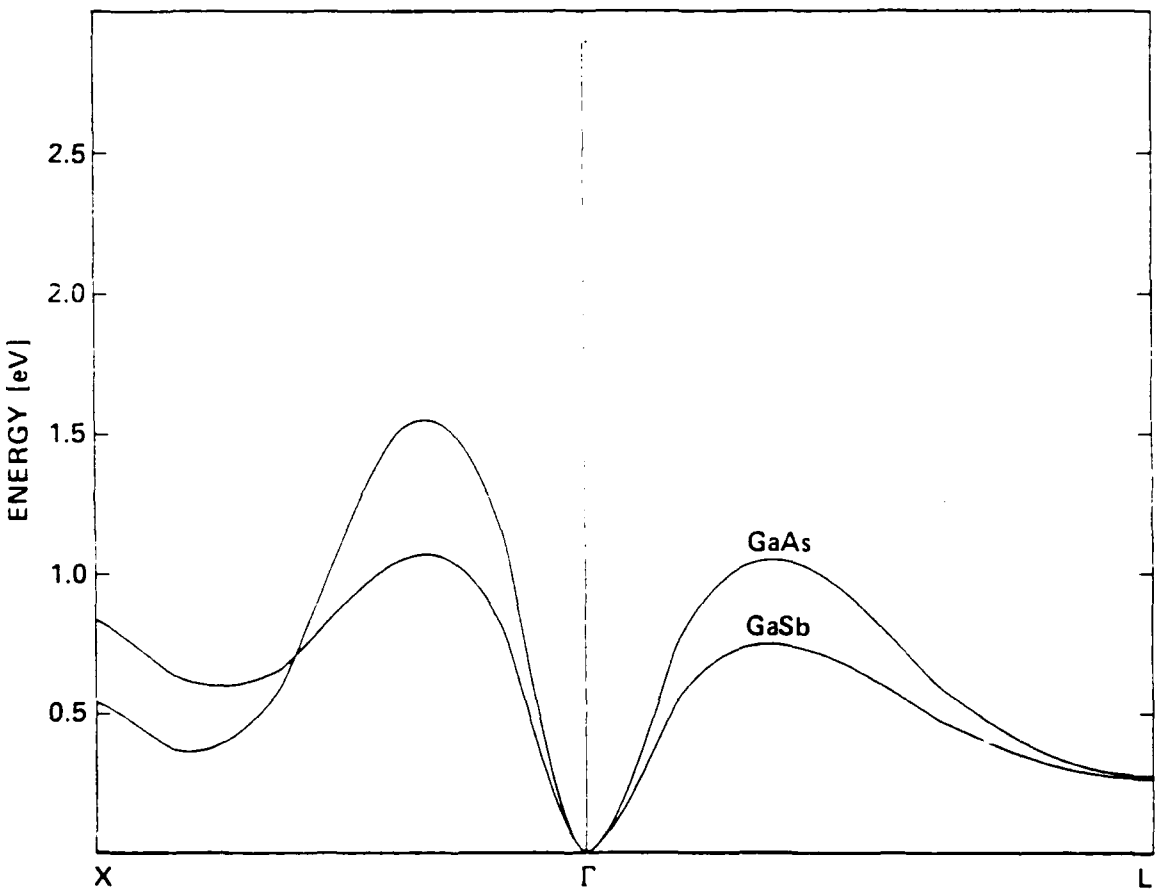

FIGURE 2b

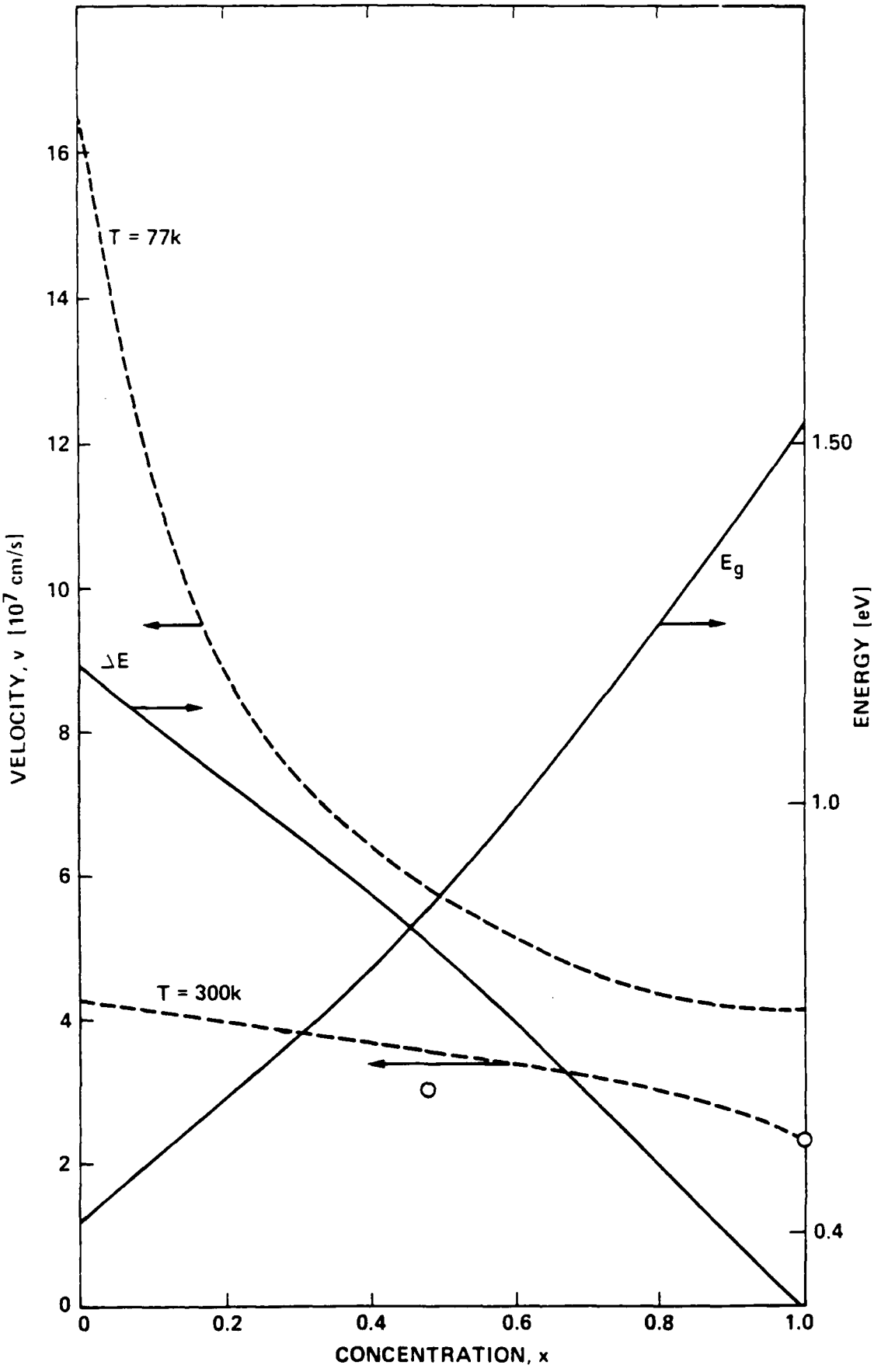
VELOCITY, v [10^7 cm/s]
ENERGY [eV]
CONCENTRATION, x
T = 77k
T = 300k
Eg
ΔE
0
2
4
6
8
10
12
14
16
0.4
1.0
1.50
0
0.2
0.4
0.6
0.8
1.0

FIGURE 3

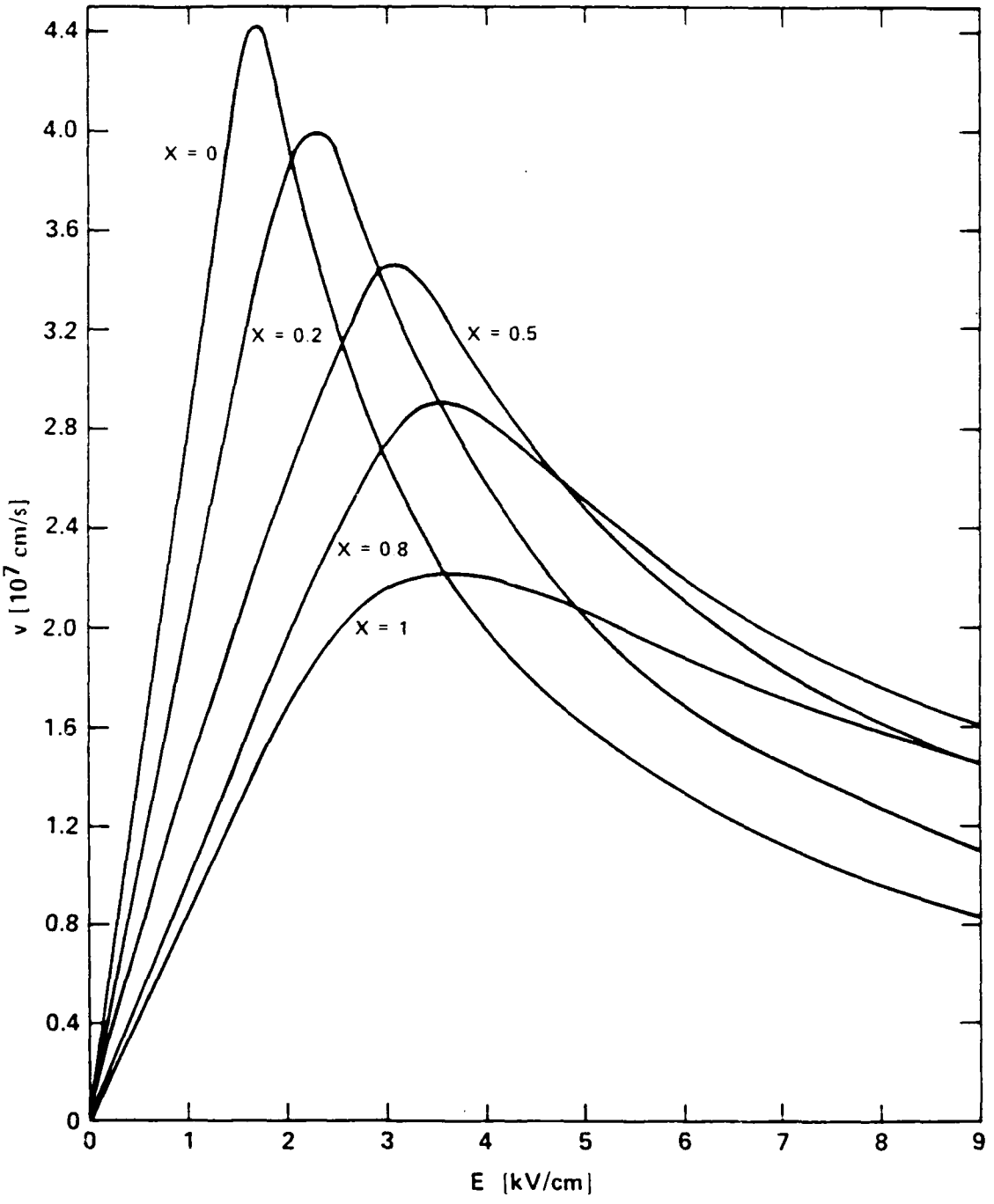
4.4
4.0
3.6
3.2
2.8
2.4
2.0
1.6
1.2
0.8
0.4
0
v [10^7 cm/s]
X = 0
X = 0.2
X = 0.5
X = 0.8
X = 1
0
1
2
3
4
5
6
7
8
9
E [kV/cm]

FIGURE 4

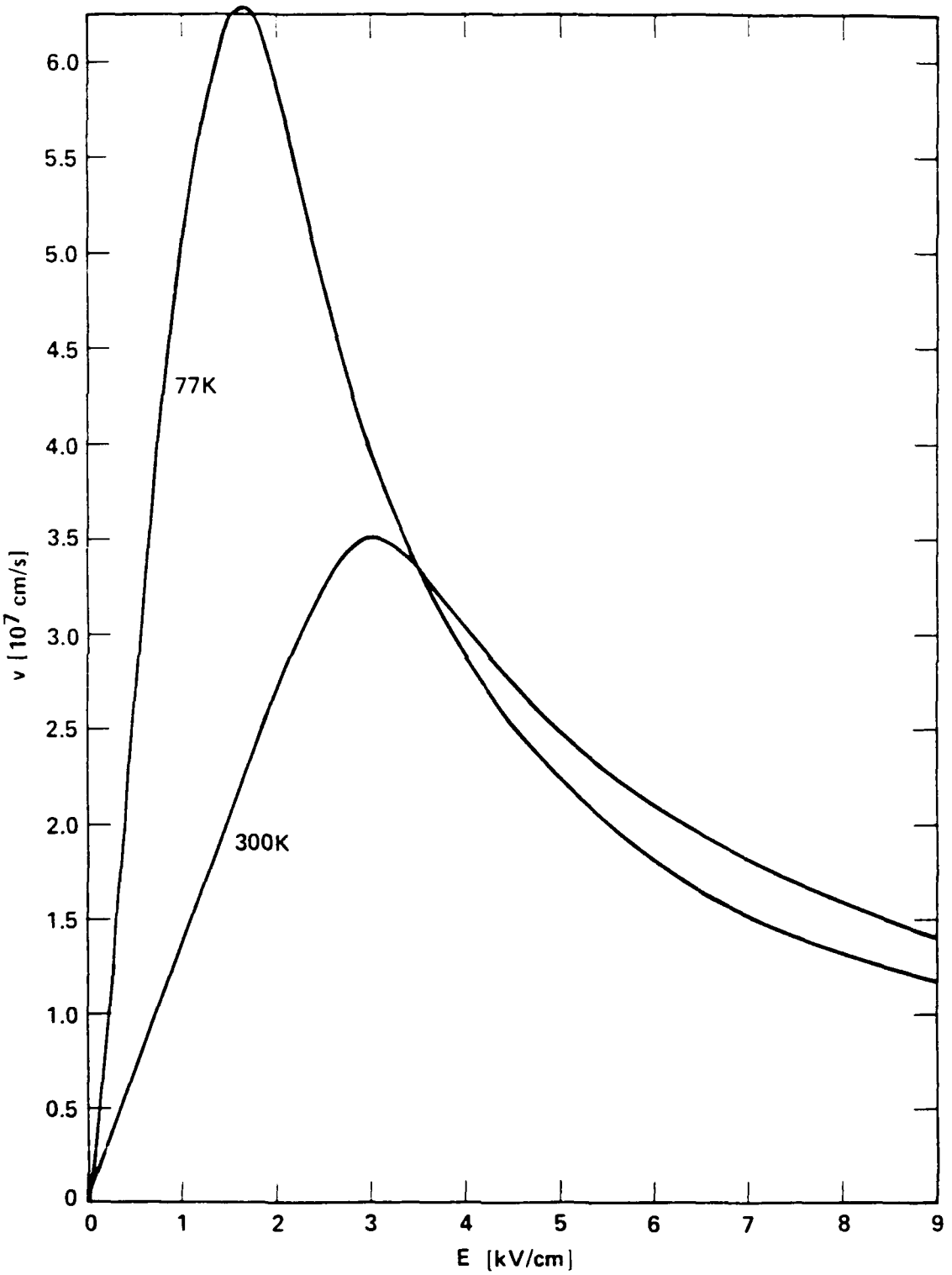
6.0
5.5
5.0
4.5
4.0
3.5
3.0
2.5
2.0
1.5
1.0
0.5
0
v [10^7 cm/s]
77K
300K
0
1
2
3
4
5
6
7
8
9
E [kV/cm]

FIGURE 5

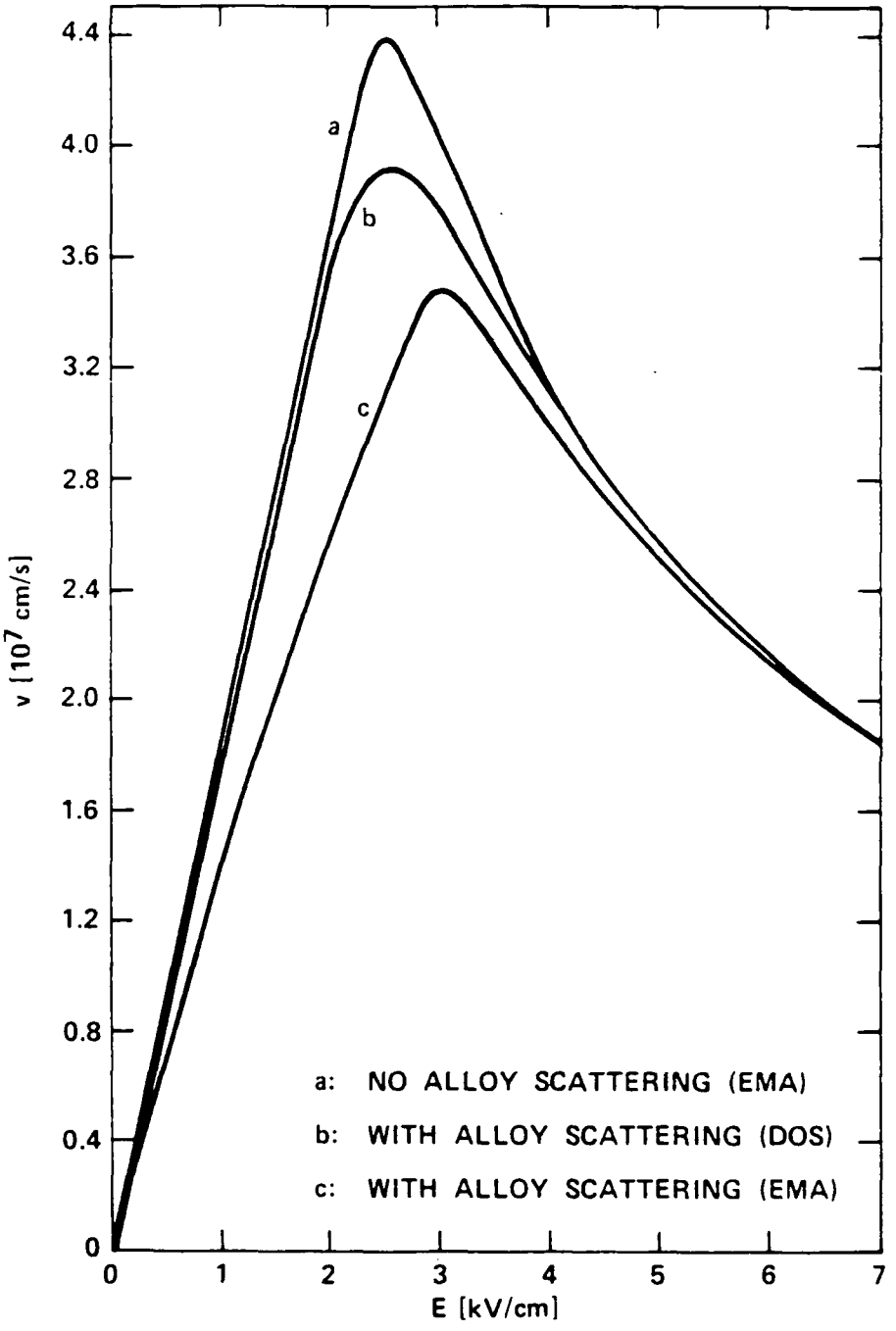
4.4
4.0
3.6
3.2
2.8
2.4
2.0
1.6
1.2
0.8
0.4
0
v [10^7 cm/s]
a
b
c
a: NO ALLOY SCATTERING (EMA)
b: WITH ALLOY SCATTERING (DOS)
c: WITH ALLOY SCATTERING (EMA)
0
1
2
3
4
5
6
7
E [kV/cm]

FIGURE 6

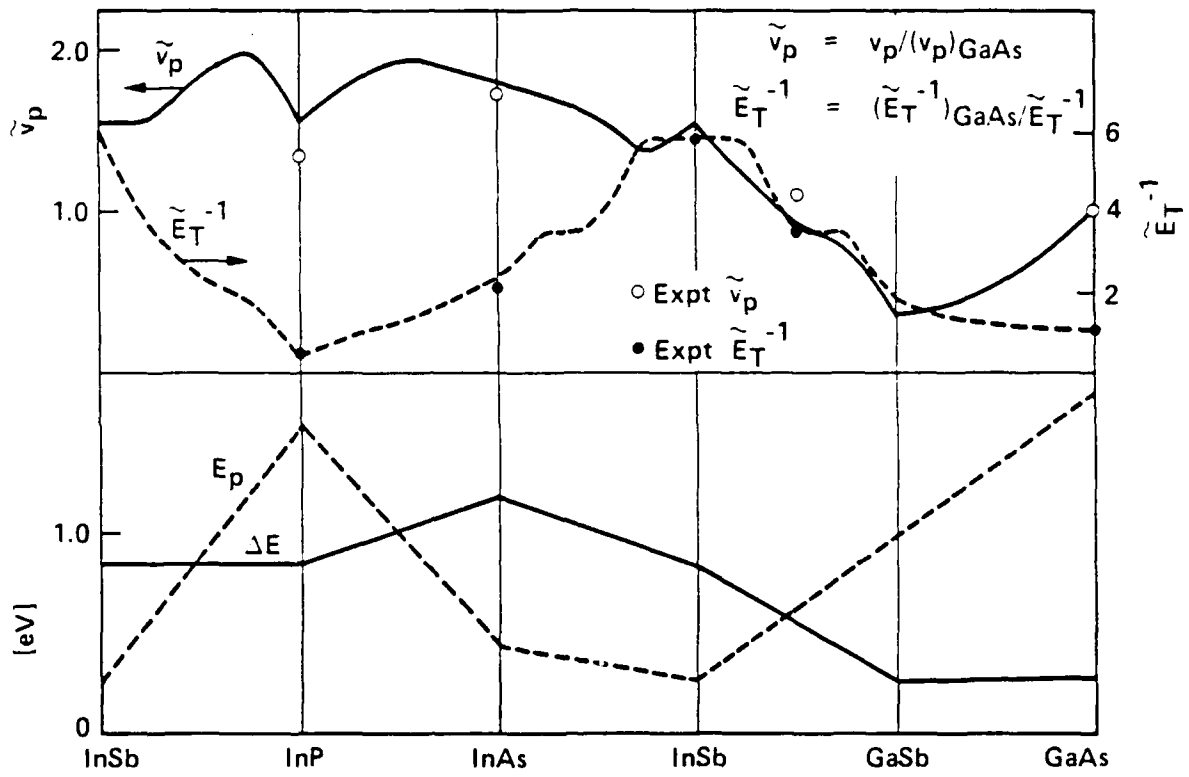
$\tilde{v}_p = v_p/(v_p)_{GaAs}$
$\tilde{E}_T^{-1} = (\tilde{E}_T^{-1})_{GaAs}/\tilde{E}_T^{-1}$
$\tilde{v}_p$
$\tilde{E}_T^{-1}$
2.0
1.0
6
4
2
Expt $\tilde{v}_p$
Expt $\tilde{E}_T^{-1}$
E_p
ΔE
[eV]
1.0
0
InSb
InP
InAs
InSb
GaSb
GaAs

FIGURE 7

Table I. Important band parameters of III-V compounds.

Parameter	GaAs	InAs	InP	GaSb	InSb
E_g(eV)	1.52	0.42	1.42	0.86	0.25
$m^*(m_o)$	0.067	0.026	0.072	0.050	0.018
ΔE(eV)	0.282	1.11	0.82	0.27	0.73
R	42.95	186.02	45.02	200.10	1493.14
E_p(eV)	1.70	0.44	1.54	0.98	1.26